



## Comparative physicochemical, thermal and microstructural properties of starches from two underutilized taro ecotypes

Nguimbou Richard Marcel<sup>1</sup>, Himeda Makhlouf<sup>1</sup>, Njintang Yanou Nicolas<sup>2\*</sup>, Tatsadjieu Ngouné Léopold<sup>3</sup>, Facho Balaam<sup>4</sup>, Scher Joel<sup>5</sup>, Mbofung Carl M.F.<sup>1</sup>

<sup>1</sup>National School of Agro-Industrial Sciences (ENSAI), University of Ngaoundere P.O. Box 455, Adamaoua, Cameroon

<sup>2</sup>Faculty of Sciences, University of Ngaoundere P.O. Box 454, Adamaoua, Cameroon

<sup>3</sup>Institut Universitaire de Technologie, Université de Ngaoundéré BP 455, Adamaoua, Cameroun

<sup>4</sup>Faculté des Sciences exactes et appliquées, Université de N'djamena, Tchad

<sup>5</sup>Laboratoire d'Ingénierie de Biomolécules (LIBio), Université de Lorraine, 2 avenue de la Forêt de Haye B.P. 172 F-54505 Vandoeuvre lès Nancy

Received: 22 March 2012

Revised: 27 March 2012

Accepted: 28 March 2012

**Key words:** *Giant taro starch, Sosso taro starch, microstructure, thermal properties, functional properties.*

### Abstract

*Egg like taro* (a giant taro consumed as food in the North West region of Cameroon) and *Sosso taro* (a smallest taro cultivated in Chad) are essential sources of starch. *Egg like* and *Sosso taro* starches were isolated and characterized by scanning electron microscope (SEM), X-ray diffraction, Differential scanning calorimetry (DSC), and functional properties. Compared with *Sosso* a common variety of *Colocasia esculenta* starch, the morphology of giant taro starch showed smaller particles. All the starch granules were irregular in shape and dissimilar in size. The crystal type of giant taro starch was A-type pattern. The amylose content in giant taro starch was 14.6%. The starch isolated from giant taro showed the highest transition temperature (71.10–85.80°C) and intermediate enthalpy (14.02–16.22J/g) of gelatinization. According to the gelling property evaluated as the lowest gelation concentration, giant taro starch exhibited higher pasting property with a very high ability to absorb water, to swell and solubilise. Taken together, the particular high swelling power of starch from giant taro opens an avenue to its industrial and home use as comminuted products including sausages, custards and dough. Further investigations are needed on the structural and rheological characterization of the starch to its optimal utilization.

\*Corresponding Author: Njintang Yanou Nicolas ✉ [njintang@yahoo.fr](mailto:njintang@yahoo.fr)

## Introduction

Taro (*Colocasia esculenta* L. Schott) is an important tuber in Cameroon which is cultivated not only for its underground tubers, but also for its leaves. Taro is usually consumed in Cameroon in the form of *achu*, as thick porridge obtained by cooking and pounding to a smooth and homogenous paste (Njintang *et al.*, 2007). The production of taro in Cameroon last to 4 million tons and occupied the second rang for tubers production after cassava and before yams (Minagri, 2006). Due to increase in population and urbanization, and integration of taro into intensive commercial chain, the corms have become an attraction for populations. In particular a new variety of taro, giant taro less known up to now, becomes an important food material for the preparation of *achu* in combination with common taro.

Giant taro is an aroid (Araceae family), as are the other taro types *Colocasia esculenta* (true or dry-land taro) and *Xanthosoma* (new world taro). Giant taro is referred in literature as *Cyrtosperma merkusii* (Englberger *et al.*, 2008), but the Cameroonian variety has not yet been identified. It is grown in swampy areas (other taros are grown on dry areas) and is large in size, growing to heights of 2 – 3 m (*Colocasia* growing to about 0.5 m). It has huge corms that usually weight 0.5 to 4 kg, but they may weigh as much as 7 kg. As other taro varieties, giant taro tubers are potential sources of flour and industrial starch that has not yet been utilized (Aboubakar *et al.*, 2008). It is therefore clear that a significant amount of work remains to be done on the functional characteristics of native taro starch if it is ever to become competitive with commercial starches such as corn, wheat and potato. Starch has many functions in home and industrial use (Les Copeland *et al.*, 2009). Botanical starch is becoming an essential part of people diet and is considered as health food because of its coming from green botanical source and its undefiled property. Now, because the single cereal starch source is insufficient to supply the starch, industry pays

attention to other alternatives could satisfy people's demands (Maneka *et al.*, 2005). From a pharmaceutical standpoint, starch finds its value in solid oral dosage forms, where it has been used as a binder, diluent and disintegrant. Also tuber starch has been applied in textile, papermaking, feedstuff and paint industry as thickening and gelling agent (Tara, 2005). Therefore, giant taro having considerable starch content may be considered as new starch sources for the food and medicine industry like other medicinal plants.

Some chemical and physical properties of taro starches have been reported on several Hawaiian (Jane *et al.*, 1992) varieties. But few have been interested on their functional properties. As far as giant taro is concerned, no study in our knowledge is reported. Recently, Aboubakar *et al.* (2008) evaluated the physicochemical, thermal properties and microstructure of six varieties of taro (*Colocasia esculenta*) flours and starches.

The aim of this study therefore was to elucidate the physicochemical, thermal and moisture sorption profile of giant taro starch and compare it to another less valorized taro variety, *Sosso*, from Chad.

## Materials and methods

### *Extraction of starch*

Giant taro and *Sosso* (Chadian taro variety) starches were isolated from the tubers collected from the North West region of Cameroon (giant taro) and South of Chad (variety *Sosso*). Giant taro was reported by farmers to be two years mature while maturity of the *Sosso* variety was 10 months. The corms were peeled and, for giant taro, the central and peripheral parts were separated before extraction according to the procedure of Sathe *et al.* (1982). In the procedure of extraction, flour (1 kg) was mixed with 10 L of distilled water contained in a bottle and the unit agitated during 30 min. The bottle was thereafter covered with aluminum foil and placed at 40°C during 5 h for the

extraction of the starch. The mixture thus obtained was centrifuged to 4500 g at 20 °C during 15 min. To the pellet obtained 10 L of a 2 % NaCl solution were added and the unit agitated during 10 min. The bottle was again covered with aluminum foil and was left to rest for 12 h before being centrifuged at 4500 g, 20°C for 15 min. The pellet was washed on several occasions with distilled water and then 0.03 M NaOH was added and the mixture kept at 4°C for 12 h. The mixture obtained was once more centrifuged during 30 min to 4500 g and the pellet was washed with water several times and sieved to pass through a 75 µm sieve mesh for the elimination of fibers. The starch obtained was centrifuged and the pellet obtained spread out over an aluminum plate and dried at  $30 \pm 2^\circ\text{C}$  during 12h. The starch thus obtained was sealed in polyethylene bags and stored at 4°C for further analysis.

#### *Chemical analysis of taro starch*

Moisture content, lipids and ash content of taro starches were determined according to the AACC (1990) standard methods. Proteins were determined after digestion with concentrated sulfuric acid followed by microtitration on an automatic microanalyser type Vapodest 4S Gerhardt, Germany (AOAC, 1999). The nitrogen was converted into protein content using the conventional factor 6.25. Amylose content of starch samples were determined following the colorimetric method described by Chrastyl (1987). In the procedure, starch samples were submitted to methanol extraction followed by solubilisation in an alkaline solution, and reaction with iodine and colorimetric measurement in a Spectronic 2PC apparatus. Phosphorus content was determined in ash samples using the blue molybdenum colorimetric method (Rodier, 1978).

#### *Starch microstructure (SEM)*

Granule morphology was examined using scanning electron microscope (SEM) according to the procedure earlier described (Aboubakar *et al.*, 2008). Scanning electron microscopy was carried out using a Leica

Stereoscan 360 SEM (LEO, Cambridge, UK) operated at an accelerating voltage of 10 kV.

#### *X-ray powder diffraction*

Structural characterization was carried out using a Siemens D5000 X-ray diffractometer (Siemens, Munich, Germany) according to the procedure described by Maneka *et al.*, (2005). Triplicate measurements were made at 20°C and the degree of crystallinity was estimated by means of the technique described by Nara and Komiya (1983).

#### *Gravimetric moisture sorption*

The Equilibrium moisture content of the taro starch was determined at 20°C according to the static gravimetric method of Wolf *et al.* (1985). The desorption isotherms were determined on samples hydrated in a glass jar over distilled water at a room temperature to approximately 30% dry basis moisture content. Samples of 1.0000 g were weighed in weighing bottles which were put in hygrometers with six saturated salt solutions, LiCl, CH<sub>3</sub>COOK, MgCl<sub>2</sub>, Mg(NO<sub>3</sub>)<sub>2</sub>, NH<sub>4</sub>Cl, BaCl<sub>2</sub>, used to obtain constant water activities environments respectively of 0.1131, 0.2311, 0.3307, 0.5438, 0.7923 and 0.903 (Bell and Labuza, 2000). All the salts used were of reagent grade. At high water activities ( $a_w > 0.70$ ) crystalline thymol was placed in the hygrometers to prevent the microbial spoilage of the flour. The hygrometers were kept in thermostats at  $20.0 \pm 0.2$  °C. Samples were weighed (balance sensitivity  $\pm 0.0001$  g) every three days. Equilibrium was acknowledged when three consecutive weight measurements showed a difference less than 0.001 g. The moisture content of each sample was determined by the oven method (105 °C for 24 h) by means of triplicate measurements.

#### *Isotherm modeling*

The GAB (Guggenheim-Anderson-De Boer) equation of desorption was exploited to describe the change in moisture as a function of water activity. The GAB

model is applied for water activity ranging from 0.05 to 0.95 according to the formula:

$$X = \frac{M_0 \cdot C \cdot K \cdot a_w}{[(1 - K \cdot a_w) \times (1 - K \cdot a_w - C \cdot K \cdot a_w)]}$$

In this equation, X is the equilibrium moisture content,  $M_0$  is the monomolecular moisture content of the product, C is a constant link to the temperature.

#### *Colour measurements*

Colour measurements of flour samples were carried out using a portable tintometer (Lovibond RT Colour Measurement Kit V2.28) with a 10° observer window and a D-65 light source as described earlier by Kaptso *et al.* (2008).

#### *Water solubility index and water absorption capacity*

Water solubility index (WSI) was measured according to the method described earlier (Njintang *et al.*, 2001). A 2.5 g sample of starch was dispersed in 25 mL of distilled water; special care was taken to break up any lumps using a glass rod. After 30 min of stirring, the dispersion was rinsed into tarred centrifuge tubes made up to 32.5 mL and then centrifuged at 3000 g for 10 min. The supernatant was then decanted and the weight of its solid content determined after it had been evaporated to a constant weight. The WSI was then calculated as weight of dissolved solids in supernatant to that of dry flour sample.

The water absorption capacity expressed in percent was calculated as weight of water retained in the pellet after centrifugation to that of its corresponding dry solid.

#### *Least gelation concentration and retrogradation index determination*

The least gelation concentration (LGC) was estimated according to the method described by Coffman and Garcia (1977). Samples of starch, 2–18% (w/v), were prepared in test tubes with 5 mL of distilled water. The starch suspensions were mixed with a Vari-whirl mixer for 5 min. The test tubes were heated for 30 min at 80 °C in a water bath, followed by rapid cooling under

running cold tap water. The test tubes were further cooled at 4 °C for 2 h. LGC was determined as that concentration when the sample from the inverted test tube did not fall down or slip. After that, the test tubes were kept at 4°C inside the refrigerator for 8 days. Following this period of storage, the samples were centrifuged at 5000 g for 15 min. The volume of the supernatant was measured to determine the retrogradation index (RI) as the percentage of water syneresis from the paste. The retrogradation index was calculated according to the formula:

$$RI = \frac{V}{V_1 + V_2} \times 100$$

In this equation, RI is the retrogradation index expressed in mL/100mL, V is the volume of syneresis,  $V_1$  is the volume of reconstitution (5 mL),  $V_2$  is the moisture content of the product.

## **Results and discussion**

### *Chemical Composition of starches*

As shown in Table 1, protein and lipid contents of taro starches ranged from 0.69 to 2.46 % and from 0.07 to 0.24 % (dry-weight basis), respectively. This revealed the high purity of taro starches. The amylose content of taro starch varied with the variety and ranged from 14.1 to 27.6 %. These values are comparable to those reported for other tropical tubers such as cassava (13.6-23.8 %), sweet potatoes (8.5-38 %), *Xanthosoma* (15-25 %), *Dioscorea* (12.5-29.7 %), *Colocasia* (3-43 %) (Moorthy, 2002). The wide variation reported for starches give evidence of such influencing factors as variety, stage of maturity, agro-ecological zone, planting season. The present work revealed that giant taro exhibited lower amylose content. The difference in the amylose content may be due to the difference in tubers age with older exhibiting lower amylose content. Phosphorus content varied from 0.13 to 0.17 %, values which are significantly higher than those reported in literature for taro (0.006 to 0.013 %) and other tubers (Moorthy, 2002). The high phosphorus content is well known to impart high viscosity to starch and also improve the gel strength. High phosphorus starches

can find use in food applications requiring high gel strength, such as jellies etc.

**Table 1.** Chemical composition of starch samples

	Giant taro, central part	Giant taro, peripheral part	Sosso taro
Moisture (g/100g)	8.23 ± 0.14 <sup>a</sup>	8.21 ± 0.13 <sup>a</sup>	7.83 ± 0.04 <sup>b</sup>
Ash (g/100g)	0.20 ± 0.09 <sup>a</sup>	0.32 ± 0.10 <sup>a</sup>	0.35 ± 0.01 <sup>d</sup>
Proteins (g/100g)	2.46 ± 0.21 <sup>a</sup>	2.24 ± 0.31 <sup>a</sup>	0.69 ± 0.01 <sup>c</sup>
Lipids (g/100g)	0.15 ± 0.47 <sup>b</sup>	0.24 ± 0.01 <sup>a</sup>	0.07 ± 0.01 <sup>c</sup>
Amylose (g/100g)	15.1 ± 0.1 <sup>a</sup>	14.1 ± 0.7 <sup>a</sup>	27.6 ± 0.4 <sup>b</sup>
Phosphorus (g/100g)	0.13 ± 1.9 <sup>a</sup>	0.17 ± 5.7 <sup>c</sup>	0.15 ± 1.0 <sup>b</sup>

Means ± SD; n=3; values with different letters within the same row differed significantly (p<0.05).

**Table 2.** Colour and crystallinity characteristics of giant and Sosso taro starches.

Properties	Giant taro central part	Giant taro peripheral part	Sosso taro
L*	84.9 ± 0.10 <sup>a</sup>	85.2 ± 0.06 <sup>b</sup>	98.7 ± 0.56 <sup>c</sup>
a*	0.87 ± 0.03 <sup>a</sup>	0.81 ± 0.04 <sup>a</sup>	1.39 ± 0.24 <sup>b</sup>
b*	2.81 ± 0.05 <sup>a</sup>	2.64 ± 0.06 <sup>a</sup>	3.37 ± 0.81 <sup>b</sup>
Degree of crystallinity (%)	20.49	21.03	27.40
Relative crystallinity (%)	25.78	26.64	37.69

Means ± SD; n=3; values with different letters within the same row differed significantly (p<0.05).

#### Microstructure of taro starches

Scanning electron micrographs of giant taro and Sosso taro starches are shown in Fig. 1. All starch samples exhibited irregularly shaped, tiny granules with polyhedral edges and interparticulate variability. These specific characteristics of taro starches have been reported recently (Aboubakar, 2009). In addition the size of taro granules is less than 5 µm, but much lower

for giant taro (Fig 1A and 1B) than for Sosso variety (Fig 1. C).

#### Colour of taro starches

Colour is an important criterion for starch quality, especially for use in textile industries. The starch paste should be clear and free from any off-colour for better acceptability (Moorthy, 2002). Starch from taro tubers has a white color as referred to the color coordinates shown in Table 2. Sosso sample has a colour whiter than that of giant taro. The color of starch has been link to the method of extraction, the plant source and treatment. In this respect starch from cassava tubers has been reported to have a good white colour, if the skin and rind are removed prior to crushing. In addition it has been shown that *Colocasia* has a brown colour and is considerably improved by use of ammonia during extraction (Moorthy, 2002).

#### X-ray power diffraction of taro starches

The crystal characterizations of native starch granules are often carried out using X-ray diffraction patterns, which had been classified as A, B or C pattern. According to current models of starch granule, parallel double amylopectin molecules result in the formation of crystalline regions, while amylose molecules result in the formation of amorphous regions in the starch structure (Cheetham and Tao, 1998). All starch samples showed strong diffraction peaks at 17°, 19° and 27° which was consistent with expected A-type pattern (Fig. 2). Although tuber starches usually give a B-type powder pattern, the characteristic peak for B-pattern at 5° 2 theta is seen neither for giant taro, nor for Sosso starch. According to Hizukuri (1986), starches with amylopectin of short chain length (< 20 residues) exhibit 'A' type crystallinity, whereas those with amylopectin of longer average chain length show the 'B' pattern. More over there is increasing evidence that the crystalline nature of starch is due to amylopectin, while amylose disrupts the order of the crystallites (Cheetham and Tao, 1998). The degree of crystallinity was higher for sosso taro variety compared

to the giant taro variety (Table 2). These values are lower than those of some other tropical tubers such as Tacca (35 %), potato (46 %), tapioca (48 %). However our results are inconsistent with the theory that higher amylose content (variety) corresponds to a lower

crystalline order (giant taro variety). This implied that the amylose content is not the only component contributing to the three dimensional structure of the starch, but also others such as phosphorus.

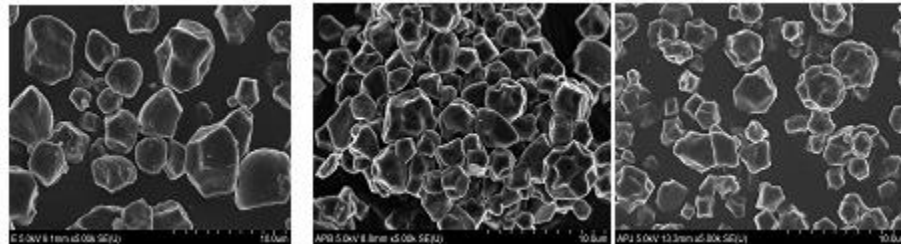


**Fig. 1.** Microstructure of starches from Sosso taro (A) and giant taro peripheral (B) and central (C) parts.

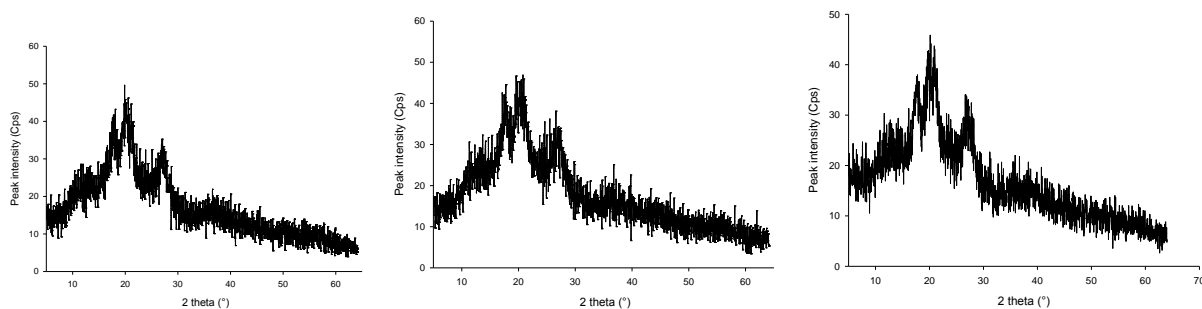


**Fig. 2.** X-ray diffraction of giant taro central (A) and peripheral (B) sections and Sosso taro (C) starches.

**Table 3.** Thermal properties of taro starches.

	$T_o$	$T_p$	$T_f$	$E_o$ (J/g)
Giant taro inner part	$62.2 \pm 0.49^b$	$85.8 \pm 0.42^b$	$88.8 \pm 0.49^b$	$14.0 \pm 0.29^a$
Giant taro external part	$52.8 \pm 1.66^a$	$71.1 \pm 0.42^a$	$75.8 \pm 0.49^a$	$16.2 \pm 0.35^b$
Sosso taro	$76.2 \pm 0.34^e$	$84.5 \pm 0.32^e$	$93.2 \pm 0.35^e$	$16.3 \pm 0.21^e$

Means $\pm$ SD; n=3; values with different letters within the same column differed significantly ( $p < 0.05$ ).

**Table 4.** The GAB coefficients ( $K_b$ , C and  $M_o$ ) and coefficient of determination ( $R^2$ ) of the adsorption isotherm modeling of taro starches.

Taro variety/section	$K_b$	C	$M_o$ (g/100g)	$R^2$
Giant taro central section	0.65	22.2	6.5	0.93
Giant taro peripheral section	0.51	14.7	13.3	0.95
Sosso taro	0.81	14.0	8.8	0.83

#### *Thermal characteristics of taro starches*

The thermal properties of taro starches are shown in Table 3. As expected, only a single endothermic peak is

exhibited by the three samples at high water content (volume fraction of water 0.70). This continuous endothermic transition is indicative of granule swelling

and crystallite melting occurring over the gelatinization range. The onset ( $T_o$ ), peak ( $T_p$ ), and end ( $T_f$ ) temperatures of gelatinization of giant taro starch were observed to be lower than that of *Sosso* taro starch. The results obtained from the X-ray diffraction studies indicated that the degree of crystallinity of giant taro starch is lower than that of *Sosso* taro starch. Moreover, the enthalpy of gelatinization for giant taro starch is lower than that of *Sosso* taro starch. Thus it was suggested that *Sosso* taro starch has more crystalline regions that are thermally and structurally stable as compared to giant taro starch. These observations contrasted however with the amylose content which was high for *Sosso* variety. These results are in accordance with the water absorption ability which was significantly higher for giant taro than for *Sosso* taro starch (Fig. 3). The results from the water absorption behavior studies substantiate the fact that the associative forces, that stabilize the granule structure in giant taro starch, are weaker than those in *Sosso* taro starch.

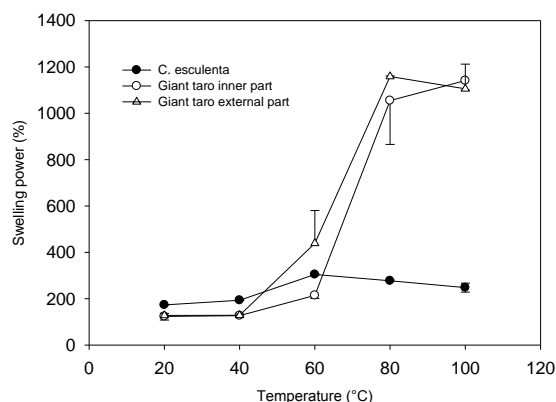


**Fig. 3.** Swelling power of taro starches.

#### Water absorption ability of taro starches

WAC represents the ability of a food system to associate with water under conditions of varying water content during preparation. The water absorption capacity of starch samples increased as the incubation temperature increased. As been known, starch could not absorb cool water due to its crystal structure. The starch molecules started to integrate with water as the

temperature increased, then the amylose and amylopectin were dissociated in suspension, and the solubility of starch was increased, the insoluble starch granules started to absorb and swell. It can be seen from Fig. 3 that taro samples absorbed slowly from 40°C to 60°C, and quickly from 60°C to 80°C. In a comparative basic, giant taro absorbed water at high temperature 6 times more than *Sosso* variety and others varieties reported in literature (Aboubakar *et al.*, 2008). The high water absorption capacity of giant taro starch offers particular technological use as gelling and thickening agent.

**Table 5.** Least gelation concentration and retrogradation index of taro starches.

	Least gelation concentration (g/mL)	Retrogradation index (mL/100 mL)
Giant taro central part	5	3.0 ± 0.1 <sup>a</sup>
Giant taro peripheral part	4	2.0 ± 0.1 <sup>a</sup>
<i>Sosso</i> taro	10	7.0 ± 0.1 <sup>b</sup>

Means±SD; n=3; values with different letters within the same column differed significantly ( $p < 0.05$ ).

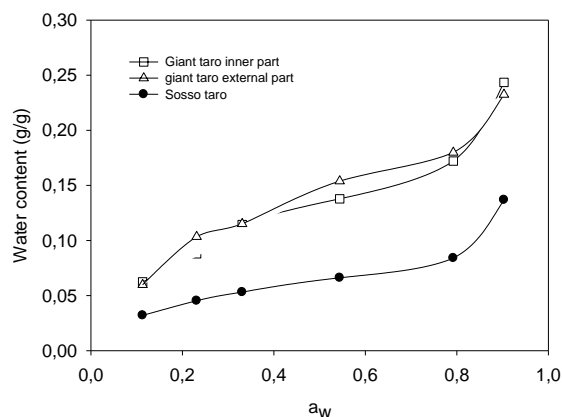


**Fig. 4.** Adsorption isotherms of taro starches.

The ability of taro starch to absorb water was also evaluated and expressed as variation of moisture with water activity ( $a_w$ ) at 20°C (Fig. 4). The figure indicated that variation in the moisture content of starches

depends on the relative humidity (RH) of the atmosphere in which they have been stored. The shape of the curves is sigmoid, showing one inflection point, which has been reported to characterize materials with high sugars content (Maskan and Gögüs, 1997). Such material samples present typical curve with three different regions (Chungcharoen and Lund, 1987): region 1, corresponding to  $a_w < 0.2$ , which relates to adsorption of monomolecular film of water, region 2 for  $a_w$  range of  $0.22 - 0.7$ , corresponding to adsorption of additional layers over this monolayer, and region 3 for  $a_w$  range of  $0.7 - 0.99$  corresponding to condensation of water in the pores of the material followed by dissolution of soluble material (Benado and Rizvi, 1985). The adsorption curves confirm the high ability of giant taro starch to hold water as shown earlier with the evaluation of water absorption capacity.

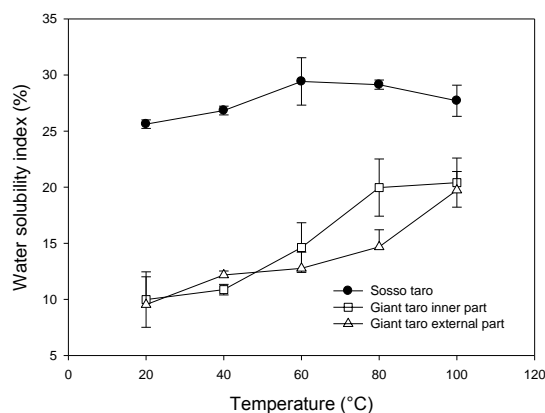


**Fig. 5.** Water solubility index of taro starches.

The GAB model was used to explain the sorption of taro starch presented in Fig. 4. The coefficients ( $M_0$ ,  $C$  and  $k_0$ ) of this model are given in Table 4 with the determination coefficient ( $R^2$ ). The determination coefficients were all higher than 80 % suggesting that the experimental results fitted well to the GAB model. The monolayer moisture content ( $M_0$ ), considered as that corresponding to the amount of water adsorbed at specific sites are 6.5 (Giant taro central part), 13.3 (Giant taro peripheral part) and 8.8 (Sosso taro). The higher monolayer moisture level suggested the higher

amorphous character of the starch granules, and hence its hygroscopicity. The monolayer moisture content determined in this study is significantly higher than that reported for potatoes starch (2.1-3.7%, Al-Muhtaseb *et al.*, 2004). This result confirms once more the high ability of giant taro starch to fix water as shown earlier. Significant variation was observed on the constant  $k_b$  which ranges from 0.51 to 0.65 (Giant taro) and 0.81 (Sosso taro). Relatively high  $k_b$  values (range 0.88-0.89) have been reported for high amylose and high amylopectin potatoes starch (Al-Muhtaseb *et al.*, 2004). The most important change observed on the GAB model parameters was on the surface energy constant ( $C$ ).  $C$  value significantly varies with taro section and variety varying from 14.0 (Sosso taro) to 22.2 (Giant taro central section). As equally reported in literature, the most varying constant of the GAB model with temperature is  $C$  which decreases as the temperature increases (Peng *et al.*, 2007). According to Labuza (1975) type II isotherm generally exhibited  $C$  values between 2 and 50, while values higher (range 50-200) reflected type I isotherm with significant chemisorption. This observation suggested that in giant taro (especially central section) starch, the surface energy constant of starch granule is high. This remark confirms the high gelatinization temperature determined by DSC.

#### Water solubility ability

Fig. 5 showed that the solubility slightly increased with the increase in temperature from 20 to 80°C. The solubility of Sosso taro starch was much higher than that of giant taro starch. Giant taro starch exhibited very low solubility at 20°C and formed only a temporary suspension when stirred in water. According to Eliasson and Gudmundsson (1996), the low solubility of starches at low temperatures could be attributed to the semi-crystalline structure of the starch granules and the hydrogen bonds formed between hydroxyl groups in the starch molecules. As expected the maximum solubility (15% for giant taro and 27% for Sosso taro) reached by the different

samples at higher temperature reflects the amylose contents of the samples.

#### *Least gelation concentration and retrogradation index of taro starches*

Gelation properties of taro starches are presented in Table 5. The least gelation concentration (LGC), used as the index of gelation, indicated that all native taro starch samples exhibited high gelation ability. In particular giant taro exhibited lower values. According to Lawal and adebowale (2005) gel strength depends on strength of intragranular binding forces within swollen starch granules. In this respect it can be believe that intragranular bonding forces are higher in giant taro starch. And since gel formation in starches entails swelling and hydration of starch granules, which occurs predominantly in the amorphous region of starches, it is reasonable to say that giant taro starch are more amorphous than *sozzo* variety. This observation corroborated results from the water absorption capacity and gelatinization profile.

One important observation on the gel obtained from giant taro is its low retrogradation index. In fact 3 to 5 mL of water exudates from 100 mL of giant taro gel during storage, while the corresponding value was 10 mL for *sozzo* variety. Retrogradation is characterized by the molecular interactions (hydrogen bonding) between starch chains after cooling of the gelatinized starch paste (Hoover, 2001). During this phenomenon, amylose forms double helical associations of 40–70 glucose units whereas amylopectin crystallization occurs by association of the outermost short branches (Singh et al. 2003). The amylose content has been reported to be one of the influential factors for starch retrogradation. In this respect a greater amount of amylose has traditionally been linked to a greater retrogradation tendency in starches (Whistler and BeMiller, 1996). In addition the retrogradation has been reported to be accelerated by the amylopectin with larger amylose chain length (Singh et al. 2003). The low level of amylose in giant taro has probably contributed to its low retrogradation index.

In general, taro starch is characterized by its high ability to absorb water (Onyeike *et al.*, 1995; Nip, 1997). This property may impart its structural property characterized by its granules size less than 5  $\mu\text{m}$ . Among taro varieties, giant taro starch is characterized by granules of more less sizes and water absorption capacity higher than 10 g water/g starch. This parameter is of particular interest in home and industrial preparation such as comminuted products including sausages, custards and dough where water holding capacity is an important functional trait in foods so as to improve handling characteristics and maintain freshness.

#### **Acknowledgment**

The authors wished to thank the Cooperation pour la Recherche Universitaire (CORUS, FRANCE) for financial support.

#### **References**

- AACC. 1990.** American Association of Cereal Chemists. Approved methods of the AACC (7th ed.). St. Paul, MN.
- Aboubakar, Njintang YN, Scher J, Mbofung CMF. 2008.** Physicochemical, thermal properties and microstructure of six varieties of taro (*Colocasia esculenta* L. Schott) flours and starches. Journal of Food Engineering **86**, 294–305.
- Aboubakar, Njintang YN, Scher J, Mbofung CMF. 2009.** Texture, microstructure and physicochemical characteristics of taro (*Colocasia esculenta*) as influenced by cooking conditions. Journal of Food Engineering **91**, 373–379.
- Al-Muhtaseb AH, McMinn WAM, Mage TRA. 2004.** Water sorption isotherms of starch powders Part 1: Mathematical description of experimental data. Journal of Food Engineering **61**, 297–307.

**AOAC. 1999.** Official Methods of Analysis of AOAC international, 16th Ed.

**Bell LN, Labuza TP. 2000.** Moisture Sorption: Practical Aspects of Isotherm Measurement and Use, second ed. AACC, Saint Paul.

**Benado AL, Rizvi SSH. 1985.** Thermodynamic properties of water on rice as calculated from the reversible and irreversible isotherms. *Journal of Food Science* **50**, 101–105.

**Cheetam NWH, Tao L. 1998.** Solid state NMR studies on the structural and conformational properties of natural maize starches. *Carbohydrate Polymers* **36**, 285–292.

**Chrastyl J. 1986.** Amélioration technique et économique du procédé de fabrication de l'amidon aigre de manioc. Rapport final du contrat CEE/STD2 TS2A-0225, CIRAD, Montpellier, France, P. 49.

**Chungcharoen A, Lund DB. 1987.** Influence of solutes and water on rice starch gelatinization. *Cereal Chemistry* **64**, 240–247.

**Coffman CW, Garcia VV. 1977.** Functional properties and amino acid content of a protein isolate from mung bean flour. *Journal of Food Technology* **12**, 473–484.

**Eliasson AC, Gudmundsson M. 1996.** Starch: Physicochemical and functional aspects. In A. C. Eliasson (Ed.). *Carbohydrates in food* (pp.431–503). New York: Marcel Dekker.

**Englberger L, Schierle J, Kraemer K, Aalbersberg W, Dolodolotawake U, Humphries J, Grahame R, Reid PA, Lorens A, Alberta AK, Levendusky A, Johnson E, Paul Y, Sengebau F. 2008.** Carotenoid and mineral content of Micronesian giant swamp taro (*Cyrtosperma*)

cultivars. *Journal of Food Composition and Analysis* **21**, 93–106.

**Hizukuri S. 1986.** Polymodal distribution of the chain length of amylopectin and the crystalline structure of starch granules. *Carbohydrate Research* **147**, 324–347.

**Hoover R. 2001.** Composition, molecular structure, and physicochemical properties of tuber and root starches: a review. *Carbohydrate Polymers* **45**, 253–267.

**Jane J, Shen L, Lim S, KaseMSuwantt, Nip WK. 1992.** Physical and Chemical Studies of Taro Starches and Flours. *Cereal Chemistry* **69**, 528–535.

**Kaptsso KG, Njintang YN, Komnek AE, Hounhouigan J, Scher J, Mbofung CMF. 2008.** Physical properties and rehydration kinetics of two varieties of cowpea (*Vigna unguiculata*) and bambara groundnuts (*Voandzeia subterranea*) seeds. *Journal of Food Engineering* **86**, 91–99.

**Labuza TP. 1975.** Interpretation of sorption data in relation to the state of constituent water. In R. Duckworth (Ed.), *Water relations in foods*. New York: Academic Press pp. 155–172.

**Les Copeland, Blazek J, Salman H, Tang CM. 2009.** Form and functionality of starch. *Food Hydrocolloids* **23**, 1527–1534.

**Maneka VR, Kunle OO, Emeje OM, Builders P, Rama Rao VG, Lopez PG, Kolling MW. 2005.** Physical. Thermal and Sorption Profile of Starch Obtained from *Tacca leontopetaloides*. *Starch/Stärke* **57**, 55–61.

**Maskan M, Gögüs F. 1997.** The fitting of various models to water sorption isotherms of pistachio nut paste. *Journal of Food Engineering* **33**, 227–237.

- Minagri. 2006.** Evolution de la production de quelques cultures vivrières, *Institut National de la Statistique - Cameroun en Chiffres*.
- Moorthy SN. 2002.** Physicochemical and functional properties of tropical tuber starches: A review. *Starch* **54**, 559-592.
- Nara S, Komiya T. 1983.** Studies on the relationship between water saturated state and crystallinity by the diffraction method for moistened potato starch. *Starch/Stärke* **30**, 111-114.
- Nip WK. 1997.** Taro. In: Smith DS (ed) *Processing vegetable and technology*, 1st edn. Technomic Publishing, Lancaster, Pennsylvania, USA pp. 355-387.
- Njintang NY, Mbofung CMF, Waldron KW. 2001.** In Vitro Protein Digestibility and Physicochemical Properties of Dry Red Bean (*Phaseolusvulgaris*) Flour: Effect of Processing and Incorporation of Soybean and Cowpea Flour. *Journal of Agriculture and Food Chemistry* **49**, 2465-2471.
- Njintang YN, Bouba AA, Mbofung CMF, Aboubakar, Bennett RN, Parker M. 2007.** Biochemical characteristics of taro (*Colocasia esculenta*) flour as determinant factors of the extend of browning during Achu Preparation. *Journal of Food Technology* **2**, 60 - 70.
- Onyeike NE, Olungwe T, Uwakwe AA. 1995.** Effect of heat-treatment and defatting on the proximate composition of some Nigerian local soup thickeners. *Food Chemistry* **53**, I73- I75.
- Peng G, Chen X, Wu W, Jiang X. 2007.** Modelling of water sorption isotherm for corn starch. *Journal of Food Engineering* **80**, 562-567.
- Rodier J. 1978.** L'analyse de l'eau: chimie, physico-chimie, bactériologie. 6ème édition du Dunod. Technique, Paris, France, P. 1136.
- Sathe PD, Deshpande SS, Salunkhe DK. 1982.** Isolation and partial characterisation of black gram (*Phaseolus mango* L.) starch. *Journal of Food Science* **47**, 1524-1527.
- Singh N, Singh J, Kaur L, Singh SN, Singh GB. 2003.** Morphological, thermal and rheological properties of starches from different botanical sources Review. *Food Chemistry* **81**, 219-231.
- Tara A. 2005.** Modification chimique de l'amidon par extrusion réactive. Thèse présentée à l'Ecole Supérieure d'Ingénieurs en emballage et conditionnement, Reims, France, P. 190.
- Tester RF, Morrison WR. 1990.** Swelling and gelatinization of cereal starches: Effect of amylopectin, amylose and lipids. *Cereal Chemistry* **67**, 551-557.
- Whistler RL, BeMiller JN. 1996.** Starch. In: R. L. Whistler & J. N. BeMiller (Eds), *Carbohydrate chemistry for food scientists* (pp. 117-151). St. Paul, MN: Eagan Press.
- Wolf W, Spiess WEL, Jung G, Weisser H, Bizot H, Duckworth RB. 1985.** The water-vapor sorption isotherms of microcrystalline cellulose and purified potato starch: Results of a collaborative study. *Journal of Food Engineering* **3**, 51-73.